Semantics of the Visual Environment Encoded in Parahippocampal Cortex

Michael F. Bonner[1], Amy Rose Price[1], Jonathan E. Peelle[2], and Murray Grossman[1]

Abstract

■ Semantic representations capture the statistics of experience and store this information in memory. A fundamental component of this memory system is knowledge of the visual environment, including knowledge of objects and their associations. Visual semantic information underlies a range of behaviors, from perceptual categorization to cognitive processes such as language and reasoning. Here we examine the neuroanatomic system that encodes visual semantics. Across three experiments, we found converging evidence indicating that knowledge of verbally mediated visual concepts relies on information encoded in a region of the ventral-medial temporal lobe centered on parahippocampal cortex. In an fMRI study, this region was strongly engaged by the processing of concepts relying on visual knowledge but not by concepts relying on other sensory modalities. In a study of patients with the semantic variant of primary progressive aphasia (semantic dementia), atrophy that encompassed this region was associated with a specific impairment in verbally mediated visual semantic knowledge. Finally, in a structural study of healthy adults from the fMRI experiment, gray matter density in this region related to individual variability in the processing of visual concepts. The anatomic location of these findings aligns with recent work linking the ventral-medial temporal lobe with high-level visual representation, contextual associations, and reasoning through imagination. Together, this work suggests a critical role for parahippocampal cortex in linking the visual environment with knowledge systems in the human brain. ■

INTRODUCTION

The human brain constructs knowledge representations of objects in the visual environment. We use this information to categorize objects in perception, to refer to objects in language, and to reason about objects in thought. It remains unclear, however, how this semantic content is represented in the brain. Here we demonstrate that semantic knowledge of visual objects relies on information encoded in the ventral-medial temporal lobe—specifically, parahippocampal cortex.

Theories of semantic memory have often linked object concepts with the fusiform gyrus (Binder & Desai, 2011; Mion et al., 2010; Martin, 2007), an area that contributes to high-level object perception (Kravitz, Saleem, Baker, Ungerleider, & Mishkin, 2013). There is indeed strong evidence that the anterior portions of the fusiform gyrus encode object representations in semantic memory (Martin, 2007). However, a number of other regions are also frequently implicated in object semantics. These include parahippocampal and perirhinal cortices, the angular gyrus, the precuneus, and the posterior cingulate (Binder & Desai, 2011; Wang, Conder, Blitzer, & Shinkareva, 2010; Binder, Desai, Graves, & Conant, 2009; Tyler et al., 2004). Recent work has begun to elucidate the contributions of these other regions to semantic memory.

One relevant theory proposes that regions of the medial temporal lobe (which includes the hippocampus and parahippocampal, perirhinal, and entorhinal cortices) encode high-level object representations that underlie both perception and memory (Barense, Henson, & Graham, 2011; Bussey & Saksida, 2007; Murray, Bussey, & Saksida, 2007). This account is largely motivated by the strong connectivity of the medial temporal lobe with anterior portions of the ventral visual system (Kravitz et al., 2013). In particular, perirhinal cortex has received considerable attention in theories of visual-mnemonic representation (Murray et al., 2007; Suzuki & Amaral, 1994). However, parahippocampal cortex, a region just posterior to perirhinal cortex, is also well situated for processing high-level visual information and linking this information to a number of polymodal association cortices (Suzuki & Amaral, 1994). Indeed, parahippocampal cortex is commonly activated in studies of concrete semantics (Wang et al., 2010; Binder et al., 2009; Wise et al., 2000; Thompson-Schill, Aguirre, D'Esposito, & Farah, 1999), and it contains similar codes for object categories across both vision and language (Fairhall & Caramazza, 2013). Although this evidence suggests that parahippocampal cortex may be another critical node in the semantic network that underlies knowledge of the visual environment, it has received comparatively little attention in theories of semantic memory.

Here we examine the semantic representations of words with strong visual associations and demonstrate that

[1]University of Pennsylvania, [2]Washington University in St. Louis

parahippocampal cortex encodes visually weighted semantic knowledge. Our approach is similar to previous work examining the concreteness and imageability of words (Binder, Westbury, McKiernan, Possing, & Medler, 2005; Sabsevitz, Medler, Seidenberg, & Binder, 2005), but it differs in that we characterize semantic associations in specific sensory modalities (i.e., visual, auditory, and motor). In three experiments, we find that (1) neural activity in parahippocampal cortex is strongly engaged by the processing of visual concepts but not by concepts in other sensory modalities, (2) gray matter atrophy of parahippocampal cortex in patients with the semantic variant of primary progressive aphasia is associated with a specific impairment on visual semantics, and (3) the structure of parahippocampal cortex in healthy adults relates to individual differences in the processing of visual concepts.

METHODS

General Methods

Overview

We examined the neural basis for visual semantic processing in three experiments. In Experiment 1, we characterized the functional neuroanatomy of visually weighted lexical semantics using fMRI in healthy adults. In Experiment 2, we examined the anatomic basis for impairments on visually weighted semantic knowledge in patients with the semantic variant of primary progressive aphasia (svPPA). In Experiment 3, we identified individual differences in structural neuroanatomy in healthy adults that relate to individual variability in the processing of words that depend on visual semantic information. For all three experiments, we used the same lexical-semantic task, which allowed us to test for converging anatomic findings across studies. Furthermore, because we used verbal materials rather than images in our experiments, we were able to examine stored object knowledge separate from the perceptual processes that underlie object vision.

Word Association Task

The core experimental task in the three studies below was a two-alternative forced-choice task, similar in structure to the Pyramids and Palm Trees test, a standard neuropsychological assessment of semantic memory (Howard & Patterson, 1992). In this task, participants indicated which of two word choices "best goes with" an index word. For example, given the index word *pencil* and the choices *crayon* and *spoon*, participants should choose *crayon*. Slight variations of this task were created to accommodate the procedure for the fMRI and patient experiments, as detailed below.

All stimuli (n = 88 triads of words) were nouns, and no words were repeated in the task. We obtained the stimuli from a set of 489 nouns probed in a norming study with 22 young adults in which words were rated on a scale from 0 to 6 for how strongly they were associated with semantic features in each of three modalities: visual, auditory, and motor manipulation (Bonner, Peelle, Cook, & Grossman, 2013; Bonner & Grossman, 2012). Subsets of 22 triads were created to exhibit weightings for visual (e.g., index: diamond; target: gold; foil: lake), auditory (e.g., index: thunder; target: downpour; foil: rocket), or motor manipulation features (e.g., index: pencil; target: crayon; foil: spoon), and we also created a set of abstract trials that included words with low ratings on all three modalities (e.g., index: saga; target: epic; foil: proxy). Distributions and pairwise scatter plots of the feature ratings for all subsets are illustrated in Figure 1. The distribution plots were generated through kernel density estimation using a Gaussian kernel and Scott's rule of thumb for bandwidth selection (Scott, 2015). The stimuli are listed in Appendix A, and their psycholinguistic characteristics are summarized in Table 1. These subsets were matched on letter length, lexical frequency (Francis & Kucera, 1982), and "semantic associativity" values of the index–target and index–foil pairs (all pairwise comparisons $p > .2$). Semantic associativity values were determined in a norming study in which 16 young adults rated all index–target and index–foil word pairs for how semantically associated they were with one another on a scale of 0–6. These ratings were used to balance the difficulty of answer choices across conditions. Concreteness and imageability ratings from the MRC Psycholinguistic Database were available for 60% of the stimuli, which we report in Table 1 (Coltheart, 1981; Gilhooly & Logie, 1980; Paivio, Yuille, & Madigan, 1968). In the patient study, we focused on two of these subsets (the visual and abstract subsets), as described in Experiment 2. In the fMRI study, we combined the stimuli across all subsets and used a parametric modulation analysis to model the BOLD activation for semantic feature associations in the visual, auditory, and motor modalities (details of this analysis are described in Experiment 1).

During testing, participants saw triads of words and indicated by button press which of two answer choices below "best goes with" the index word above. Half of the target responses were on the left and half on the right. There were an equal number of left and right responses across categories, and the stimuli were presented in a random order. We administered a practice session before all experiments to familiarize participants with the task and to ensure that task instructions were understood. The practice session for the fMRI experiment was presented outside of the scanner before imaging. Participants received feedback about their responses only in this practice session and not during administration of the experimental task. Stimulus items in the practice session were not presented in the experimental trials. We used E-Prime 2.0 to present stimuli and record responses for all experiments (Psychology Software Tools, Inc., Pittsburgh, PA).

MRI Image Acquisition

Participants were scanned on a Siemens 3.0T Trio scanner (Berlin, Germany). We acquired T1-weighted structural

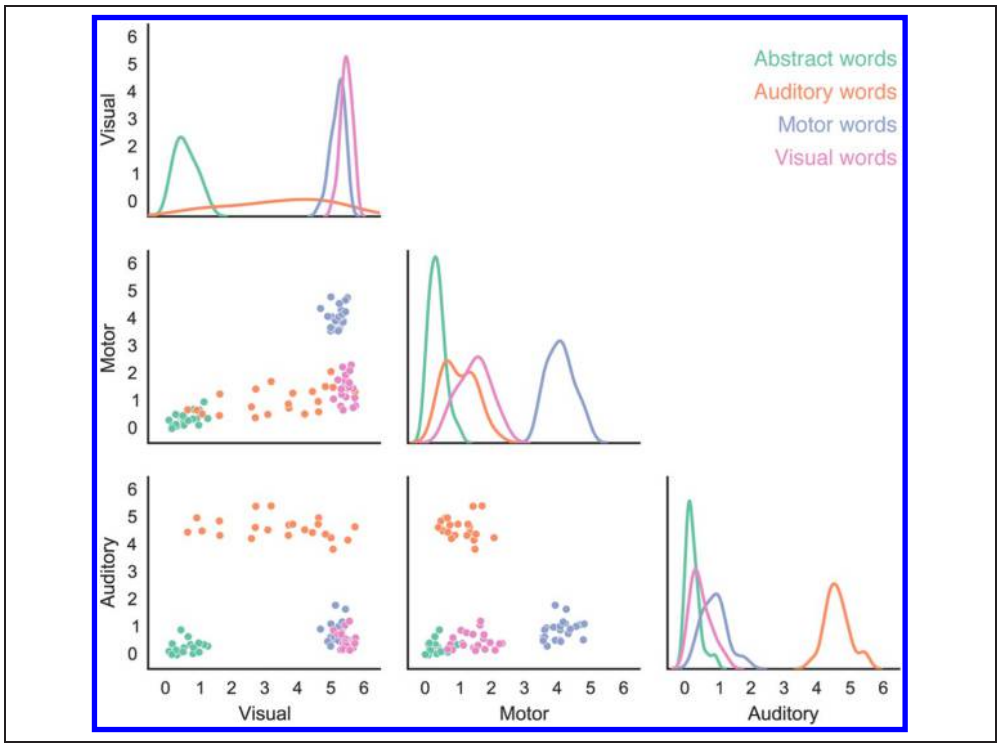

Figure 1. Distributions and scatter plots of feature ratings for all word stimuli. Feature ratings were on a 0–6 scale. Plots in the off-diagonal cells show pairwise relationships between modalities of feature ratings. Plots in the on-diagonal cells illustrate the distributions of feature ratings for each modality.

images using an MPRAGE protocol (repetition time = 1620 msec, echo time = 3 msec, flip angle = 15°, 1 mm slice thickness, 192 × 256 matrix, voxel size = 0.98 × 0.98 × 1 mm). In healthy adults, we also collected BOLD fMRI images (repetition time = 3 sec, effective echo time = 30 msec, flip angle = 90°, 64 × 64 matrix, 3 mm isotropic voxels, with fat saturation).

Experiment 1: Functional Neuroimaging in Healthy Adults

Participants

Eighteen healthy young adults from the University of Pennsylvania community participated in the fMRI study (10 women; mean age = 23.5 years, *SD* = 2.4 years). All were right-handed, and all were native English speakers with no history of neurological difficulty as determined by a preexperiment screening procedure. Two participants were later excluded (as explained in the Neuroimaging Methods section below). The demographics of the remaining participants were as follows: 9 women, mean age = 23.4 years, *SD* = 2.5 years. All participants completed an informed consent procedure approved by the University of Pennsylvania institutional review board.

Word Association Task

The word association task described above was administered to participants in the fMRI scanner.

Letter-matching Task

In the fMRI study, participants also performed a letter-matching task on triads of pronounceable pseudowords. This task was included as a low-level baseline to assess overall lexical-semantic activation in the fMRI study. There were 22 trials in this task with no repeated stimuli. The pronounceable pseudowords were matched to the real-word stimuli on letter length ($t(328) = 0.34$, $p > .7$). Each triad contained an index stimulus at the top of the screen with two answer choices below (a target and a foil). Participants indicated by button press which of the two choices ended with the same letter as the index. Half of the target responses were on the left and half on the right.

Functional Neuroimaging Methods

Experimental procedure. Participants performed both the word association task and the pseudoword letter-matching task, which served as a low-level baseline. Trials from these two tasks were interspersed in a random order. Each trial was composed of two 3000-msec events. In the first event, participants saw a blank white screen for 2000 msec, followed by a 1000-msec presentation of the task name, which was "Word Match" for the word association task and "Letter Match" for the letter-matching task. In the second event, a word or pseudoword triad appeared on the screen for 3000 msec, during which time participants indicated their answer choice by button press. A quarter of all trials were 3000-msec null events.

Table 1. Properties of the Stimulus Set

Stimulus Characteristics	*Visual*	*Abstract*	*Auditory*	*Manipulable*
Visual association ratings (scale: 0–6)	5.5 (0.3)	0.6 (0.6)	3.5 (1.8)	5.2 (0.3)
Auditory association ratings (scale: 0–6)	0.5 (0.5)	0.3 (0.3)	4.6 (0.7)	0.9 (0.5)
Motor manipulation association ratings (scale: 0–6)	1.5 (0.8)	0.4 (0.4)	1.1 (0.8)	4.1 (0.5)
Letter length	6.4 (1.8)	6.5 (2.0)	6.9 (2)	6.2 (2.2)
Lexical frequency	16 (24)	16 (18)	16 (20)	15 (24)
Semantic associativity of target (scale: 0–6)	4.3 (0.8)	4.3 (0.8)	4.5 (0.7)	4.8 (0.7)
Semantic associativity of foil (scale: 0–6)	0.4 (0.6)	0.6 (0.5)	0.8 (0.8)	0.6 (0.7)
Concreteness (scale: 100–700)	601 (21)	325 (49)	531 (90)	591 (38)
Imageability (scale: 100–700)	598 (26)	370 (62)	570 (74)	581 (38)

fMRI analysis. We processed and analyzed BOLD fMRI images using SPM8 (Wellcome Trust Centre for Neuroimaging, London, UK) and MATLAB (R2013a Mathworks; The MathWorks, Natick, MA). For each participant, the functional images were realigned to the first image (Friston et al., 1995), coregistered with the structural image (Ashburner & Friston, 1997), and normalized to standard Montreal Neurological Institute space using unified segmentation with resampling of images into isotropic 2-mm voxels (Ashburner & Friston, 2005). We inspected movement parameters generated during image realignment. One participant who moved more than 1.5 mm during the scan was excluded from further analyses. No other participants moved more than 1 mm during the entire scan. We removed low-frequency drifts by applying a high-pass filter with a cutoff period of 90 sec, and we modeled autocorrelations with a first-order autoregressive model. The images were spatially smoothed using a 10-mm FWHM isotropic Gaussian kernel.

We used a general linear model to calculate parameter estimates for each variable and to perform linear contrasts for comparisons of interest. In a single model, we modeled the fMRI BOLD responses to the word match and letter match trials (i.e., the word and pseudoword tasks) and included parametric modulators for the visual, auditory, and motor associations of each word trial. These three parametric modulators were created from the average values of the visual, auditory, and motor associations in each triad. The parametric modulators were modeled with serial orthogonalization in the following order: auditory, motor, and visual. This orthogonalization approach means that the effect for the visual parametric modulator reflects variance that is uniquely accounted for by visual associations and not by auditory or motor associations or by variance shared between the three regressors. (Similar results were obtained regardless of the ordering of the orthogonalized modulators.) To make inferences across participants, we entered the parameter estimates into a second-level random-effects analysis. One participant showed right-lateralized language activation (the only participant whose peak activation for the word association task was right inferior frontal cortex rather than left) and was excluded from the group level analysis.

Experiment 2: Structural Neuroimaging in Patients

Participants

Eight patients with svPPA (also known as semantic dementia) participated in the study (four women; mean age = 64.1 years, *SD* = 7.9 years). This syndrome is a variant of frontotemporal dementia and is predominantly associated with temporal lobe atrophy (Bonner, Ash, & Grossman, 2010; Hodges & Patterson, 2007; Hodges, Patterson, Oxbury, & Funnell, 1992). Patients were diagnosed according to published criteria (Gorno-Tempini et al., 2011), and diagnoses were confirmed in a consensus conference based on a review of a semistructured history, a comprehensive mental status exam, and a complete neurological exam by at least two independent, trained reviewers. The demographic and clinical characteristics of the patients are shown in Table 2. This table includes the Mini Mental State Exam, which assesses general cognitive performance (Folstein, Folstein, & McHugh, 1975); the Pyramids and Palm Trees test, which assesses semantic memory (Howard & Patterson, 1992); and a modified Rey Complex Figure test, which assesses visuospatial abilities and episodic recall (Libon et al., 2011).

Twenty-two healthy older adults performed the word association task as an age-matched control group for the behavioral analysis in patients (11 women; mean age = 60.9 years, *SD* = 7.6 years). A separate group of 38 healthy older adults were scanned as age-matched controls for the structural neuroimaging analysis in patients (17 women; mean age = 64.8 years, *SD* = 8.6 years). All participants and the legal representatives of the patients completed an informed consent procedure approved by the University of Pennsylvania institutional review board.

Table 2. Characteristics of the Patient Group

Demographic and Clinical Characteristics of Patients	*1*	*2*	*3*	*4*	*5*	*6*	*7*	*8*
Age, years	60	71	70	72	59	69	63	49
Education, years	20	12	12	14	17	22	22	16
Years from symptom onset	1	4	8	5	3	4	3	3
Months from first clinic visit	10	22	10	37	7	6	0	9
MMSE (max = 30)	18	6	25	27	28	22	27	15
Pyramids and Palm Trees: pictures (max = 52)	35	36	49	NA	26	36	44	47
Pyramids and Palm Trees: words (max = 52)	31	30	52	41	29	35	46	40
Rey Complex Figure: copy (max = 12)	11	12	9	12	10	12	12	12
Rey Complex Figure: recall (max = 12)	2	5	0	11	5	9	9	10

The Mini-Mental State Exam (MMSE) is a general assessment of cognitive impairment. The Pyramids and Palm Trees test assesses semantic memory. The Rey Complex Figure test examines visuospatial abilities and episodic recall. "Years from symptom onset" measures the number of years between the test date and the year that the patients or their caregivers reported first observing symptoms. "Months from first clinic visit" measures the number of months between the test date and the date of the patient's first visit to the neurology clinic at the University of Pennsylvania.

Word Association Task

For the behavioral study in patients, we examined performance on two subsets of words that differed strongly on their visual association ratings but were otherwise psycholinguistically matched. We refer to these subsets of stimuli as visual words (n = 22 triads; mean visual association strength = 5.5, SD = 0.3) and abstract words (n = 22 triads; mean visual association strength = 0.6, SD = 0.6). The patients and a group of age-matched controls performed the word association task as described in the General Methods.

Structural Neuroimaging Methods

Structural MRI analysis. We processed the T1-weighted structural images with Advanced Normalization Tools (stnava.github.io/ANTs/; Avants, Epstein, Grossman, & Gee, 2008). The images were inhomogeneity-corrected using the N4ITK algorithm (Tustison et al., 2010), warped to a local template space using symmetric diffeomorphic normalization, segmented into tissue probability maps without modulation using template-based priors, registered to Montreal Neurological Institute template space, and smoothed with a 12-mm FWHM Gaussian kernel. The preprocessed images were further analyzed using SPM8 and MATLAB. We analyzed overall gray matter atrophy with a two-sample t test comparing gray matter density in patients to gray matter density in the group of 38 age-matched healthy controls. We performed voxelwise regression analyses to identify brain regions where gray matter density was related to behavioral performance across individuals. As no global covariates were included, the regression results reflect differences in measured gray matter density (Peelle, Cusack, & Henson, 2012). In the patient group, we performed a regression analysis using each participant's performance on visual relative to abstract concepts (i.e., the difference in accuracy for visual and abstract trials). We also performed a regression analysis in patients using overall accuracy.

Interstudy similarity analysis. To examine the similarity of whole-brain effects across Experiments 1 and 2, we performed a nonparametric permutation test based on a previously published method for assessing the similarity of effects at corresponding cortical locations (Hill et al., 2010; Csernansky et al., 2008; Van Essen et al., 2006). This method has been used for examining the similarity of findings across hemispheres; here we used it to assess similarity across studies. Specifically, we used this method to test the hypothesis that the effects from the structural MRI study in patients are anatomically similar to the fMRI activation effects for visual semantics in healthy adults.

We first quantified interaction effects at each voxel by multiplying together the unthresholded, whole-brain statistical maps from each study. The first statistical map contains t values for the positive effects of the visual parametric modulator in the fMRI study. The second statistical map contains correlation coefficients for the relationship between gray matter density and behavior. In the case of the patient study, the behavioral measure is the accuracy difference score. We then performed a permutation test by randomizing the subject labels in the patient study (Nichols & Holmes, 2002). On each permutation, the following three procedures are performed: (1) the correlation coefficient for the patient study is recalculated at each voxel using the randomized subject labels, (2) interaction effects are recalculated by multiplying the new correlation map with the t map from the fMRI study, and (3) the value of the maximum interaction effect is selected from across all voxels. This procedure was repeated in 10,000 permutations. The value of the

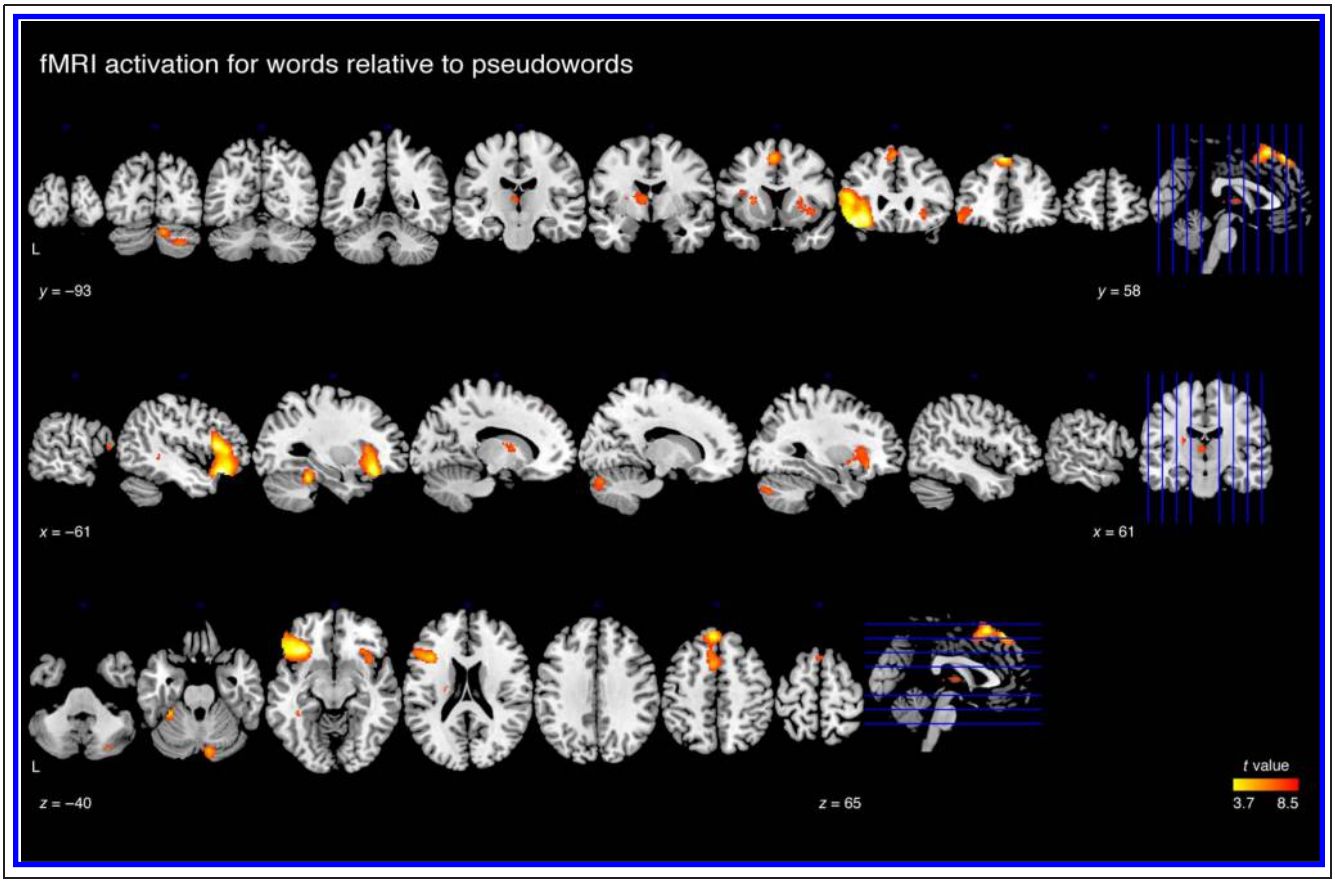

Figure 2. Overall fMRI activation for the word association task in healthy young adults. This is the activation for all word association trials relative to a baseline condition in which participants performed a letter-matching task with pronounceable pseudowords.

maximum interaction statistic at the 95th percentile across permutations corresponds to a p value of .05 corrected for whole-brain family-wise error (FWE). Note that the statistical map from the fMRI study was held constant across all permutations. This means that the test specifically assesses the probability of finding strong effects in the patient study in voxels where there are also strong effects in the fMRI study.

Experiment 3: Structural Neuroimaging in Healthy Adults

Participants and Task

These were the participants in the fMRI study in Experiment 1. We analyzed performance on the word association task (described above).

Structural Neuroimaging Methods

Structural MRI analysis. The images were processed using the same protocol as described in the Structural Neuroimaging Methods section of Experiment 2.

Visual feature sensitivity analysis. We analyzed individual differences in the behavioral performance of healthy adults on the word association task. As a group, participants showed a processing advantage for highly visual concepts. This effect was evident in participants' response latencies (see Figure 6 for plots of behavioral data). This is a common behavioral finding in studies of lexical-semantic processing and is often referred to as a concreteness effect (Paivio, 1991). For our analysis, we examined individual variability in the strength of this effect. We quantified each participant's processing advantage for visual concepts by examining the relationship between response latencies and the visual association strengths of the stimuli. We first filtered the data to remove latencies that were more than two standard deviations from the mean for all experimental conditions within each participant (mean number of trials removed = 8, SD = 1.5). As expected, there was an inverse relationship between response latencies and visual association ratings in all participants (i.e., higher visual association values were associated with shorter RTs). Using these data, we calculated a "visual feature sensitivity" score for each participant. This score was the negative correlation coefficient from a Spearman correlation of response latencies and visual association ratings. A larger value indicates a stronger behavioral advantage for visual relative to abstract concepts. We then used these values to examine the

relationship between visual semantic performance and structural neuroanatomy. To do this, we performed a correlation analysis within an ROI based on the fMRI activation cluster for visual concepts. We also performed a whole-brain regression analysis to identify voxels where gray matter density was related to individual differences in visual feature sensitivity.

Interstudy similarity analysis. We performed an interstudy similarity analysis between Experiments 1 and 3 to test the hypothesis that the whole-brain effects from the structural MRI study in healthy adults were anatomically similar to the fMRI activation effects for visual semantics. This procedure is identical to the interstudy similarity analysis described in Experiment 2, except for the fact that the structural MRI effects in the current analysis are from the individual differences data in healthy adults (rather than from the patient data). Hence, we performed 10,000 permutations with randomization of subject labels from the structural MRI study of healthy adults and quantified the probability of obtaining strong structural effects in voxels that also exhibited strong effects in the fMRI study.

RESULTS

Experiment 1: Visual Semantic Activation in Healthy Adults

We sought to identify regions where neural activity was modulated by the visual semantic information associated with words. In this fMRI experiment, healthy young adults performed a word association task and a pseudoword letter-matching task. Mean accuracy on the word task was 94.8 ± 4.9%. Mean accuracy on the pseudoword task was 98.9 ± 2.6%. We first identified regions that were activated overall during the word association task by contrasting the activation for word trials with the activation for pseudoword trials. During the word task, participants recruited a large network of lexical-semantic regions, as shown in Figure 2 ($p < .001$ voxelwise, cluster-level $p < .05$ corrected for whole-brain FWE using random

Table 3. MRI Coordinates

	Peak Coordinates					
Analysis	*x*	*y*	*z*	*Peak Location*	*Cluster Size (μl)*	*Z score*
fMRI words > pseudowords	−34	28	−12	L inferior frontal gyrus	29296	5.07
	−4	42	52	L superior frontal gyrus	7248	4.97
	−32	−40	−24	L fusiform gyrus	2496	4.73
	10	−80	−26	R calcarine sulcus	2320	4
	30	26	−10	R inferior frontal gyrus	4224	3.78
fMRI visual semantics	−30	−36	−12	L parahippocampal gyrus/collateral sulcus	2656	4.9
fMRI abstract semantics	−50	20	−12	L superior temporal gyrus	34984	5.38
	−38	−90	−2	L middle occipital gyrus	2832	4.62
	0	16	56	L/R superior frontal gyrus	7480	4.29
	−4	−20	10	L thalamus	4048	4.23
Patient atrophy	−29	−5	−34	L fusiform gyrus	93387	8.54
	48	−1	−22	R middle temporal gyrus	10194	6.13
	−17	41	11	L cingulate gyrus	1290	5.75
	54	−44	−13	R inferior temporal gyrus	910	5.44
	−31	12	32	L middle frontal gyrus	166	5.27
	−57	−57	−6	L inferior temporal gyrus	214	5.15
	−15	15	35	L cingulate gyrus	53	5.08
Patient regression analysis	−28	−32	−7	L parahippocampal gyrus/hippocampus	2660	4.11

The results for "fMRI words > pseudowords" come from the contrast of word association trials with pseudoword letter-matching trials. The results for "fMRI visual semantics" reflect the positive effects of the parametric modulator for visual association strength. The results for "fMRI abstract semantics" reflect the negative effects of the parametric modulator for visual association strength. The results for "Patient atrophy" are from the contrast of gray matter density in patients relative to controls. The results for the "Patient regression analysis" are from the regression of gray matter density and performance on visual relative to abstract concepts.

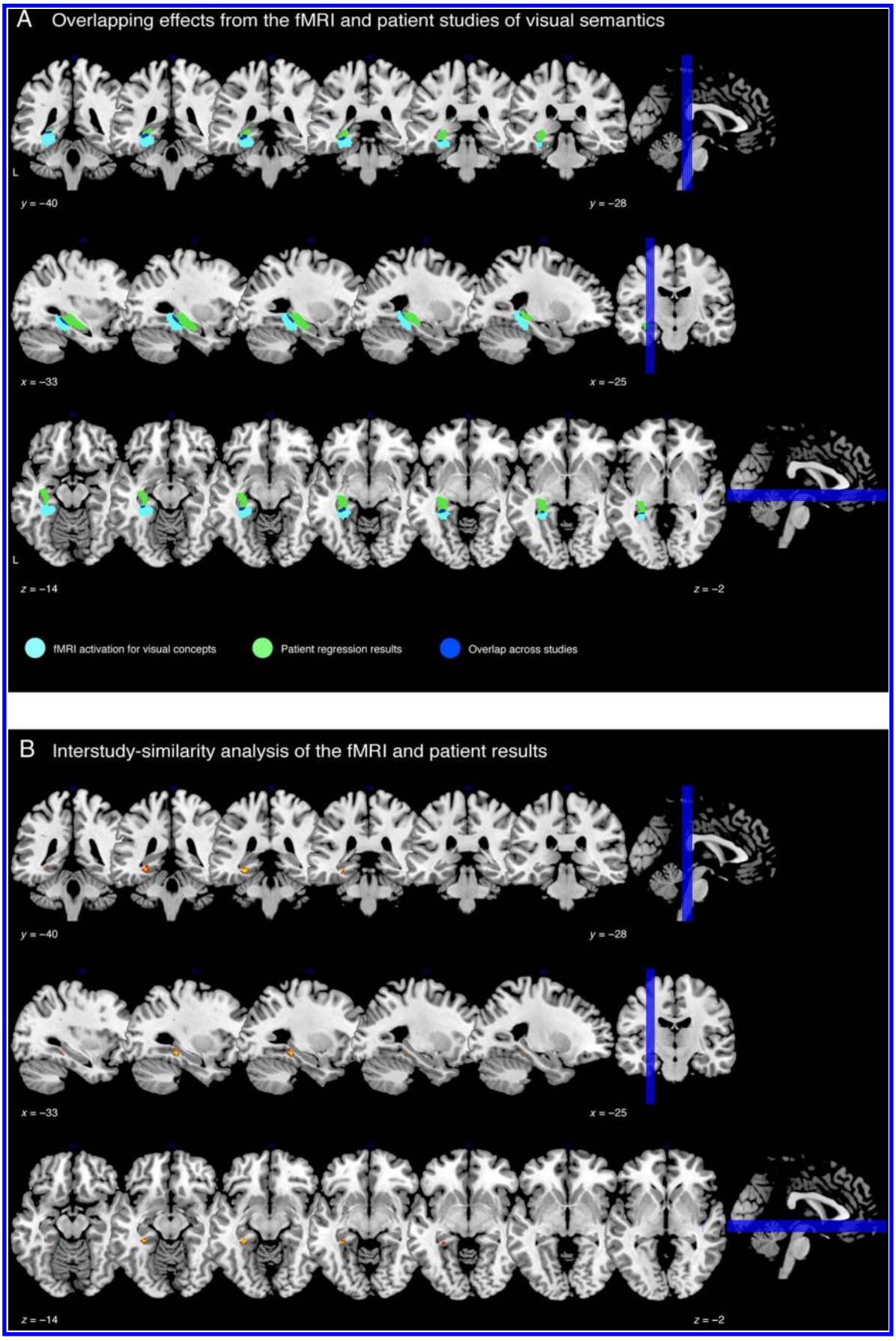
A Overlapping effects from the fMRI and patient studies of visual semantics
L
y = −40
y = −28
x = −33
x = −25
L
z = −14
z = −2
fMRI activation for visual concepts
Patient regression results
Overlap across studies
B Interstudy-similarity analysis of the fMRI and patient results
y = −40
y = −28
x = −33
x = −25
z = −14
z = −2

field theory; Worsley, Evans, Marrett, & Neelin, 1992). The coordinates for this and all other MRI analyses are listed in Table 3.

We next examined parametric modulation effects related to the visual, auditory, and motor semantic associations of the stimuli. We found that visual association strength modulated activity in regions of the left ventral-medial temporal lobe (Figure 3A; $p < .001$ voxelwise, cluster-level $p < .05$ whole-brain FWE-corrected). This cluster was centered on the collateral sulcus and parahippocampal cortex and extended into the hippocampus and fusiform gyrus. There were no other significant clusters in this analysis.

An analysis of the reverse contrast for the visual parametric modulator showed regions that were more active for abstract concepts. This was associated with activity in a large network of regions, including areas of the lateral temporal and inferior frontal lobes that are commonly implicated in language processing (Figure 4; $p < .001$ voxelwise, cluster-level $p < .05$ whole-brain FWE-corrected). There were no significant effects for the parametric modulators for auditory and motor associations.

These findings suggest that regions of the ventral-medial temporal lobe, including parahippocampal cortex, encode visual semantic information that can be accessed through language. However, a rigorous test of this hypothesis requires corroborating evidence that the representations in this region have functional implications for visual semantic behavior. Specifically, this finding leads to the prediction that atrophy of the ventral-medial temporal lobe will impair visual semantic knowledge. We examine this issue in the next experiment.

Experiment 2: Impaired Visual Semantic Knowledge in Patients

Using structural MRI, we tested the prediction that atrophy of the ventral-medial temporal lobe would result in impaired knowledge of visual concepts. We examined a rare group of patients with svPPA, a focal neurodegenerative disease associated with left-lateralized anterior ventral, medial, and lateral temporal lobe atrophy (Grossman, 2010; Hodges & Patterson, 2007). As a group, the patients in this analysis exhibited a typical pattern of gray matter atrophy for this syndrome (Figure 5; voxelwise $p < .05$ whole-brain FWE-corrected). To assess accuracy on this task, we analyzed performance on two categories of items: visual concepts and abstract concepts. Accuracy in age-matched controls was near ceiling (mean on visual concepts = 98.8 ± 0.02% and abstract concepts = 96.5 ± 0.03%). Patients were significantly impaired overall ($F(1, 28) = 76.6, p < .001$; mean on visual concepts = 77.3 ± 0.16% and abstract concepts = 72.2 ± 0.15%) and showed no group level differences across conditions. There was no main effect for stimulus category ($F(1, 28) = 3.5, p = .07$) and no interaction ($F(1, 28) = 0.52, p = .48$). t Tests showed better performance for visual relative to abstract concepts in controls ($t(21) = 2.4, p = .02$), which is a common finding (Paivio, 1991). This relative advantage for visual concepts was not significant in patients ($t(7) = 0.8$, $p = .44$).

The patients varied considerably on their relative accuracy for visual and abstract concepts. We used this variability to test the prediction that performance on visual relative to abstract concepts would be related to individual differences in gray matter atrophy of the ventral-medial temporal lobe. In a whole-brain regression analysis, we found a strong relationship between gray matter atrophy in the left ventral-medial temporal lobe and relative performance on visual concepts (Figure 3A; $p < .001$ voxelwise, cluster-level $p < .05$ whole-brain FWE-corrected, adjusted for nonstationarity). This cluster encompassed parahippocampal cortex, the hippocampus, and the collateral sulcus. There were no other significant clusters in this analysis, and there were no significant effects when we performed this contrast in the reverse direction. We also examined a whole-brain regression relating overall accuracy with gray matter atrophy, which detected no significant effects.

The finding from the regression with visual semantic performance in svPPA patients partially overlapped with the whole-brain corrected results for the visual parametric modulator in the fMRI study (Figure 3A). This overlap suggests a convergence of anatomic effects in parahippocampal cortex across the fMRI and patient experiments. However, a large portion of the whole-brain corrected cluster from the patient study includes regions that are more medial than those identified in the fMRI experiment. To further assess the overlap across these studies, we performed a whole-brain interstudy similarity analysis. This analysis quantifies the probability of finding strong overlapping effects by randomly permuting the analysis

Figure 3. Converging neuroanatomic findings for visual semantic processing in functional and structural MRI. (A) The fMRI experiment revealed one significant cluster, located in the ventral-medial temporal lobe, in which activation was parametrically modulated by the visual associations of concepts (light blue cluster). The structural MRI experiment in patients revealed one significant cluster, also in the ventral-medial temporal lobe, in which gray matter atrophy was strongly associated with a specific impairment on visual semantics (green cluster). This finding partially overlapped with the whole-brain corrected cluster identified in the fMRI experiment of healthy adults (overlap shown in dark blue). (B) An interstudy similarity analysis was performed to statistically assess the overlap of findings across the two studies (see Methods for details). This analysis quantifies the probability of finding overlapping effects by randomly permuting the analysis in the patient experiment and then finding the maximum interaction statistic with the fMRI study across all voxels on each permutation. The result is a statistical map corrected for whole-brain FWE showing voxels where there are strong effects across both studies. This analysis revealed a cluster of significantly overlapping effects in a region of the ventral-medial temporal lobe centered on the lateral aspect of parahippocampal cortex.

in the patient experiment and then finding the maximum interaction statistic with the fMRI results across all voxels on each permutation. The result is a statistical map corrected for whole-brain FWE showing voxels where there are strong effects across both studies. The interstudy similarity analysis revealed a cluster of significantly overlapping effects in a region of the ventral-medial temporal lobe centered on the lateral aspect of parahippocampal cortex (Figure 3B; $p < .05$ whole-brain FWE-corrected; cluster size: 232 μl).

Altogether, the findings from the patient experiment indicate a functional role for the ventral-medial temporal lobe in the representation of visual semantic knowledge. In conjunction with the findings from the fMRI study, these results point most consistently to the parahippocampal cortex as a critical region for visual semantics.

Experiment 3: Individual Differences in Visual Semantic Processing in Healthy Adults

The above results illustrate a critical relationship between the ventral-medial temporal lobe and knowledge of visual concepts. Here we examine whether individual differences in the neuroanatomy of this region might also relate to the performance of healthy participants (Kanai & Rees, 2011). As a group, participants from the fMRI experiment exhibited a performance advantage for visual concepts (Figure 6A), which is a common behavioral finding (Paivio, 1991). However, there was a wide range of individual differences in this effect (Figure 6B and C). We quantified the degree of each participant's performance advantage for visual concepts by measuring the relationship between their response latencies and the visual-association ratings of the stimuli. This measurement is referred to as each participant's "visual feature sensitivity." We predicted that individual differences in visual feature sensitivity would be related to individual differences in the gray matter density of parahippocampal cortex.

We tested this prediction in an ROI consisting of the activation cluster for visual semantics from the fMRI experiment (Figure 3A). Within this region, we found a significant relationship between visual feature sensitivity and the structural anatomy of parahippocampal cortex, whereby increased gray matter density was associated with stronger visual feature sensitivity scores (Figure 6D; Spearman rho = 0.68, $p = .002$). A whole-brain regression analysis showed no significant effects, but inspection of the uncorrected t maps showed a trending effect in the ventral-medial temporal lobe. We compared the similarity

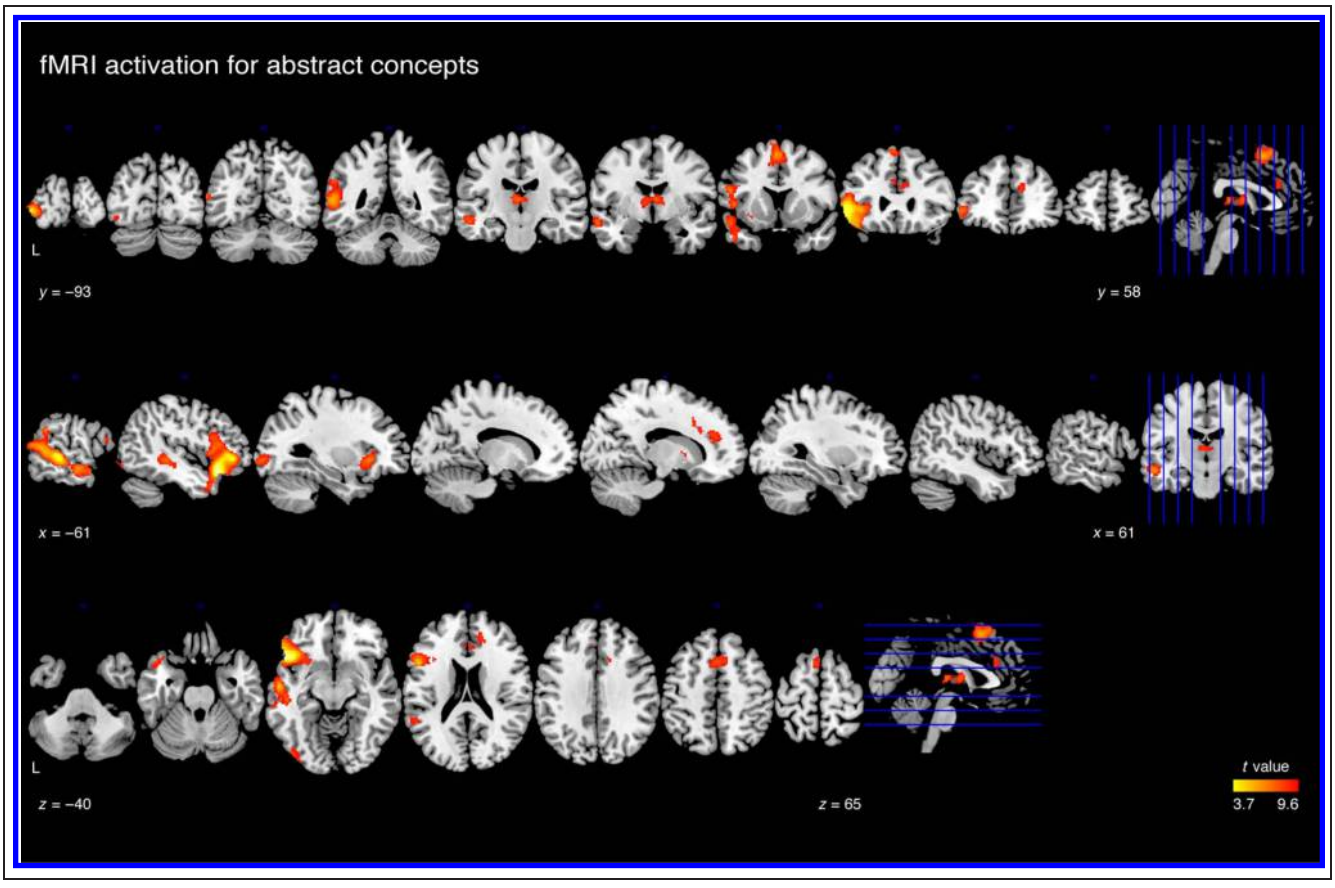

Figure 4. fMRI activation for abstract concepts in healthy young adults. These results show regions where activation was strongly modulated by the processing of abstract concepts, which have very weak associations with visual semantics.

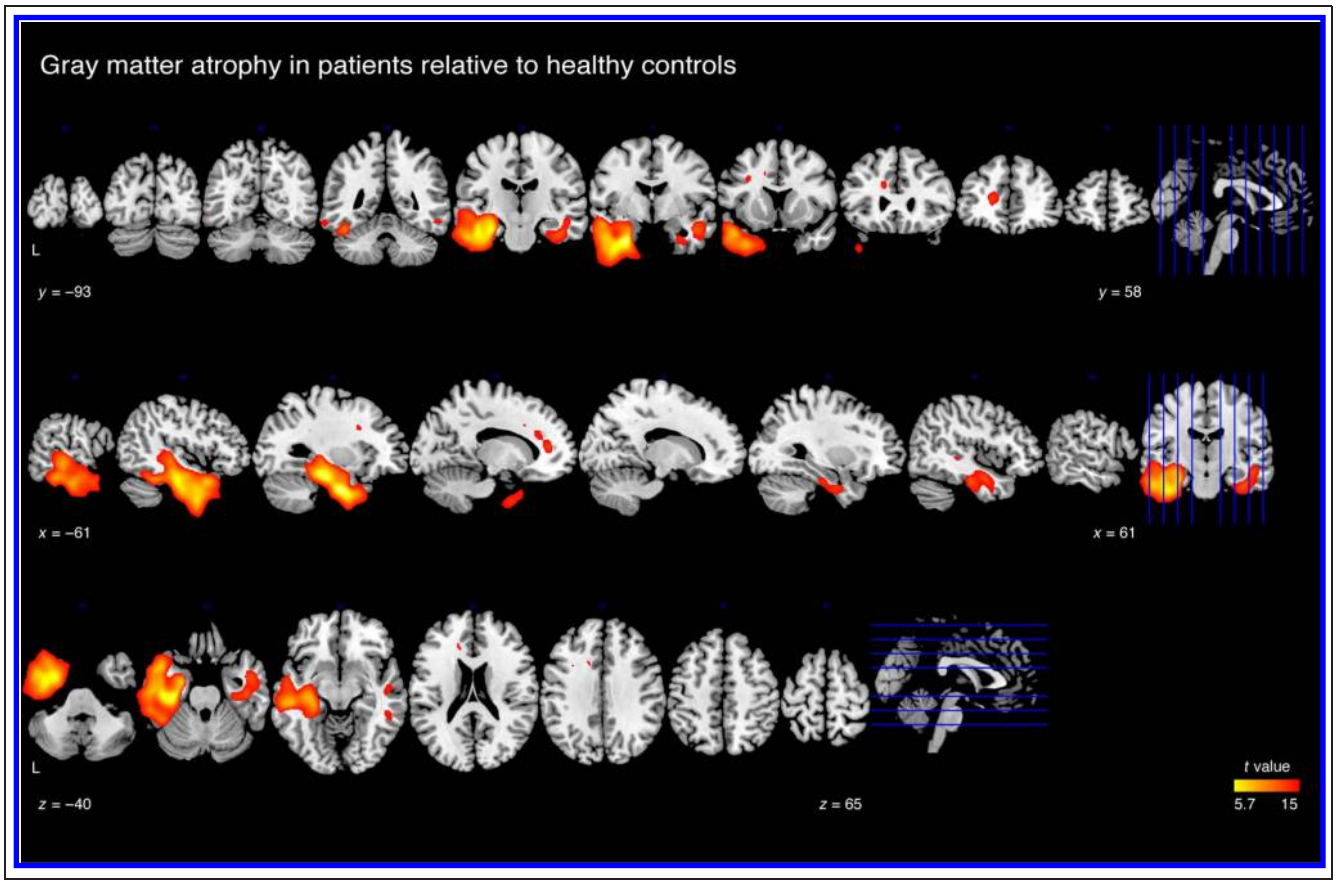

Figure 5. Gray matter atrophy in patients relative to age-matched controls. The patients have atrophy primarily affecting lateral, ventral, and medial regions of the anterior temporal lobe.

of these whole-brain effects with those from the fMRI activation results for visual semantics by performing an inter-study similarity analysis. As described above, this analysis quantifies the probability of finding strong overlapping effects across studies. This analysis revealed a cluster of significantly overlapping effects in a region of the ventral-medial temporal lobe centered on the lateral aspect of parahippocampal cortex (Figure 6E; $p < .05$ whole-brain FWE-corrected; cluster size: 464 μl). These findings demonstrate that, even in the healthy adult brain, individual differences in gray matter structure in parahippocampal cortex are related to individual differences in the processing of visual semantics.

DISCUSSION

Here we find that visual semantic knowledge relies on information encoded in parahippocampal cortex. In a series of experiments, we observed that the function and structure of parahippocampal cortex are linked to the processing of verbally mediated visual semantic information and that atrophy encompassing this region is associated with impaired knowledge of visually weighted concepts. These findings suggest that parahippocampal cortex provides a critical neural interface between visual perception and long-term semantic knowledge.

The structures of the ventral-medial temporal lobe receive major white matter projections from high-level visual association cortices (Suzuki, 1996; Suzuki & Amaral, 1994), which makes them well suited for processing complex visual information and storing this information in memory (Murray et al., 2007). Consistent with this, previous work has demonstrated the contribution of perirhinal cortex to high-level object representations, which may interface between perception and declarative memory (Barense et al., 2011; Murray et al., 2007). Indeed, perirhinal cortex receives strong projections from visual association areas TE and TEO in the monkey brain (Suzuki & Amaral, 1994). However, parahippocampal cortex is also strongly connected to high-level visual association cortices—area TF in the monkey receives ~30% of its cortical inputs from area V4 and ~10% from areas TE and TEO (Suzuki & Amaral, 1994). Furthermore, parahippocampal cortex has strong reciprocal connectivity with a large network of regions that support visual, visuospatial, mnemonic, and executive processes (Lavenex, Suzuki, & Amaral, 2002). This pattern of connectivity suggests that parahippocampal cortex processes complex visual information and interacts with a number of high-level cognitive systems.

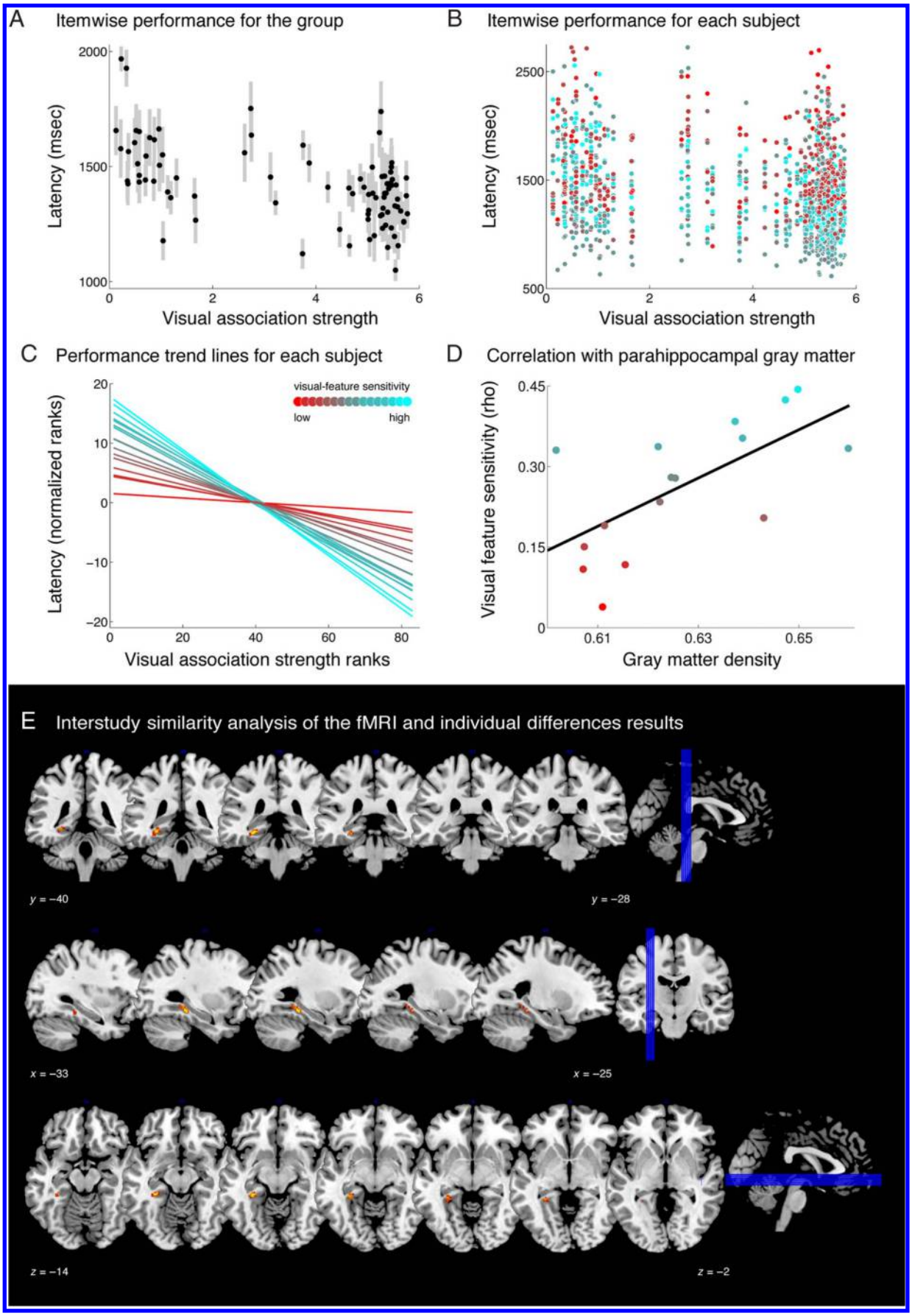
A
Itemwise performance for the group
Latency (msec)
2000
1500
1000
0
2
4
6
Visual association strength
B
Itemwise performance for each subject
Latency (msec)
2500
1500
500
0
2
4
6
Visual association strength
C
Performance trend lines for each subject
visual-feature sensitivity
low
high
Latency (normalized ranks)
20
10
0
−10
−20
0
20
40
60
80
Visual association strength ranks
D
Correlation with parahippocampal gray matter
Visual feature sensitivity (rho)
0.45
0.30
0.15
0
0.61
0.63
0.65
Gray matter density
E
Interstudy similarity analysis of the fMRI and individual differences results
y = −40
y = −28
x = −33
x = −25
z = −14
z = −2

We thus suggest that parahippocampal cortex encodes representations that support our understanding of the visual world across multiple cognitive domains, including language, vision, and long-term memory.

Although the medial temporal lobe has traditionally been characterized as supporting the formation of declarative memories (Scoville & Milner, 1957), several lines of work now indicate that this characterization is incomplete. There is a growing consensus that the medial temporal lobe contributes to numerous other cognitive functions, and cognitive theories of the medial temporal lobe may need to reconcile these disparate processes. In addition to memory formation, these medial structures have been linked with aspects of visual perception (Murray et al., 2007), mental imagery (Hassabis & Maguire, 2009; Buckner & Carroll, 2007), spatial perception (Bird & Burgess, 2008), contextual associations (Aminoff, Kveraga, & Bar, 2013), and high-level visual object representation (Barense et al., 2011). Interestingly, many of these cognitive functions rely strongly on visual information, and it has been suggested that some of these processes recruit a common mechanism for integrating high-level visual representations in perception and memory (Barense et al., 2011; Hassabis & Maguire, 2009; Buckner & Carroll, 2007; Murray et al., 2007). Our findings fit well with such an account, indicating that parahippocampal cortex contributes to knowledge of the visual world.

Some previous findings lend support to the hypothesis that parahippocampal cortex encodes semantic information. In fact, parahippocampal cortex is commonly activated in fMRI studies of semantic memory (Binder et al., 2009). Furthermore, a recent study found similar representations of object categories in parahippocampal cortex across both vision and language tasks (Fairhall & Caramazza, 2013). Despite this, few theories of semantic memory have explicitly proposed a role for parahippocampal cortex in conceptual representation (Binder & Desai, 2011; Martin, 2007; Patterson, Nestor, & Rogers, 2007). One recent study found parahippocampal cortex to be activated by multiple sensory associations when participants were deciding whether single-word concepts referred to things that could be experienced through the senses (Fernandino et al., 2015). The authors of this study propose that parahippocampal cortex functions as a multimodal hub in the semantic system. This is broadly consistent with our findings, with the exception that we did not find parahippocampal cortex to be modulated by nonvisual features. This exception may be related to the mental imagery demands of their task, which may elicit a stronger embodiment effect than that elicited by our semantic association task. Nonetheless, the diverse connectivity of parahippocampal cortex indicates that it contains information from modalities outside of vision, and our hypothesis is that its semantic representations are strongly weighted in the visual modality but are not solely visual in nature. It will be of interest in future work to examine the interaction of task demands and the modalities of information represented in parahippocampal cortex.

Another model with possible implications for semantic memory theories is the contextual association model, which proposes that parahippocampal cortex encodes the contextual associations of objects in both vision and episodic memory (Aminoff et al., 2013). Although we did not specifically probe contextual relationships in this study, our anatomic results are similar to those observed in studies of contextual associations in vision. Considering our findings and previous work implicating parahippocampal cortex in lexical semantics, it appears that the information encoded by this region is not specifically tied to context but, rather, encompasses the semantics of the visual environment more broadly.

As with many semantic effects, the semantic activation of parahippocampal cortex is likely modulated by task demands (Binder & Desai, 2011). Simple lexical tasks

Figure 6. Individual variability in parahippocampal gray matter density is related to the processing of visual semantics in healthy adults. (A) This plot shows group-averaged response latencies for each item. The dots are the group means, and the gray bars are the standard errors. At the group level, participants exhibited faster performance for concepts that are more strongly associated with visual semantics. (B) Individual participants varied in the degree of their performance advantage for visual concepts. Each participant's performance advantage was quantified as the correlation of response latency and visual association strength. This metric is referred to as "visual feature sensitivity." This scatter plot shows each participant's response latencies across all items. Participants are color coded according to their visual feature sensitivity scores, with the cooler colors indicating stronger visual feature sensitivity scores and warmer colors indicating weaker visual feature sensitivity scores. The distribution of response latencies shows that participants with higher visual feature sensitivity scores tend to have faster responses for concepts with strong visual associations. This can be seen in the clustering of blue dots at the bottom right corner of the plot. (C) This plot shows the relationship for each participant between response latency and visual association strength. Each line represents a regression within a single participant. Steeper slopes indicate faster performance for visual relative to abstract concepts. Participants varied on the extent to which they exhibited this performance advantage, as illustrated by the range of regression lines in this figure (cooler colors indicate stronger visual feature sensitivity and warmer colors indicate weaker visual feature sensitivity). (D) Individual differences in visual feature sensitivity were correlated with the gray matter density of parahippocampal cortex. The visual feature sensitivity values used in this analysis reflect the relationship between response latency and the visual association strength of the stimuli within each participant. They are calculated by taking the negative of the Spearman's rho values from a correlation of response latency and visual association strength. The gray matter density values were taken from an ROI consisting of the significant cluster from the fMRI analysis of visual semantics (see Figure 3). (E) Although there were no whole-brain corrected results for the regression analysis of visual feature sensitivity and gray matter density, inspection of the uncorrected t maps showed a trending effect in the ventral-medial temporal lobe. To explore the anatomic overlap of this effect with findings from the fMRI study of visual semantics, an interstudy similarity analysis was performed (as in Figure 3). This analysis revealed a cluster of similar effects in a region of the ventral-medial temporal lobe centered on the lateral aspect of parahippocampal cortex.

may engage only brief and sparse semantic representations that are difficult to observe with fMRI, whereas tasks involving explicit semantic judgments likely elicit stronger and more sustained activation of the semantic network. Indeed, activation of parahippocampal cortex has not always been observed in studies of concrete or visual semantics when using simple lexical decision tasks (Bonner et al., 2013; Binder et al., 2005). Here we used a task requiring explicit retrieval of semantic knowledge, which may have been helpful in detecting the contribution of parahippocampal cortex to conceptual processing.

It is worth noting that our findings do not indicate a simple embodiment of semantic knowledge through explicit simulations of perceptual processes (Caramazza, Anzellotti, Strnad, & Lingnau, 2014; Chatterjee, 2010). Rather, these findings are consistent with the idea that representations at the highest levels of the ventral visual system encode abstract stimulus associations learned over a lifetime of experience (Khaligh-Razavi & Kriegeskorte, 2014; Sha et al., 2014; Stansbury, Naselaris, & Gallant, 2013; Peelen & Caramazza, 2012) and that such representations may be accessible through modalities other than vision (Fairhall & Caramazza, 2013; Mahon, Anzellotti, Schwarzbach, Zampini, & Caramazza, 2009). Because these cortical regions encode more information than could be extracted from any given perceptual episode, the distinction between visual-perceptual processes and abstract-conceptual processes becomes blurred. In the same sense, these considerations blur the distinction between embodied and amodal theoretical accounts for our findings. Therefore, we suggest that rather than focusing on the degree to which semantic content is embodied or amodal in nature, a more useful direction for future work is to begin characterizing the computational properties that underlie such visuosemantic representations (Khaligh-Razavi & Kriegeskorte, 2014).

Previous studies of svPPA have reported relative impairments for concrete concepts (Bonner et al., 2009; Breedin, Saffran, & Coslett, 1994; Warrington, 1975) or for highly visual object concepts in particular (Hoffman, Jones, & Ralph, 2012), but there have also been exceptions noted (Hoffman & Lambon Ralph, 2011). One other study of these patients has related impairments in object semantics to an adjacent potion of the ventral-medial temporal lobe, the anterior fusiform gyrus (Mion et al., 2010). Other work has related object knowledge deficits in part to disease in the right anterior temporal lobe (Lambon Ralph, Cipolotti, Manes, & Patterson, 2010; Lambon Ralph, McClelland, Patterson, Galton, & Hodges, 2001), although we did not find evidence implicating right hemisphere regions in our studies. The results of our experiments suggest another anatomic explanation that may reconcile these apparently disparate findings. Although patients with svPPA have often been examined as a group, these patients in fact differ somewhat in the anatomic extent of their disease. The differences in cognitive findings across studies may be explained in part by differences in the underlying brain atrophy of the patients. Indeed, it has previously been suggested that individual variability in visual semantic impairments in svPPA can be accounted for by the degree of atrophy in more posterior ventral temporal regions (Hoffman et al., 2012; Hoffman & Lambon Ralph, 2011). The findings from our study appear to bear this out.

We found that individual differences in the structure of parahippocampal cortex in healthy adults are related to individual differences in the processing of visual semantic knowledge. Although previous work has indicated that individual differences in brain structure are related to variations in behavioral performance in healthy adults, this work has not focused on differences in semantic memory (Kanai & Rees, 2011). Semantic representations are often assumed to be highly similar across individuals, which is, to some extent, a prerequisite for a shared language. However, the findings from this study indicate that there may indeed be relevant individual variations in structural neuroanatomy that relate to behavioral differences in semantic-memory processing. It will be of interest in future studies to further explore how neuroanatomic differences in healthy adults can account for individual variability in semantic memory performance.

It is important to note that of the three studies presented here, only the fMRI study directly tested for neural correlates that were uniquely associated with the visual semantic modality and not the auditory or motor modalities. The patient and individual differences studies directly contrasted visual and abstract semantics, and although the results are consistent with the fMRI findings, we emphasize that the analyses are not as specific as in the fMRI study. We also note that the distribution of feature ratings differed somewhat across modalities (as can be seen in Figure 1). In particular, the ratings for the visual modality were distributed more evenly across the full range, whereas the distributions of the auditory and motor ratings had larger proportions at the lower end of the scale. These differences may have contributed to the stronger effects for the visual modality and the lack of significant findings for the auditory and motor modalities.

Finally, it is important to emphasize that visual information is only one of many feature dimensions in semantic memory. Indeed, most concepts comprise a rich network of other sensory, motor, affective, and abstract feature associations (Reilly, Peelle, Garcia, & Crutch, in press; Leshinskaya & Caramazza, 2014; Skipper & Olson, 2014; Bonner & Grossman, 2012; Kemmerer, Castillo, Talavage, Patterson, & Wiley, 2008) and may additionally rely on higher-level heteromodal association cortices, such as the angular gyrus and regions of the anterior temporal lobe, for binding and integrating these features (Price, Bonner, Peelle, & Grossman, 2015; Bonner et al., 2013; Binder & Desai, 2011; Patterson et al., 2007). Furthermore, semantic memory encompasses a broad range of relationships among concepts, including both taxonomic

associations (e.g., similar category membership) and thematic associations (e.g., complementary roles in an event). The studies presented here have not examined the possible differential roles of taxonomic or thematic information, and it will be important in future work to quantify how categories of semantic features and relationships interact.

In summary, our findings indicate that parahippocampal cortex is critical for representing semantic knowledge of the visual environment, and they are consistent with the hypothesis that the ventral-medial temporal lobe encodes visual-mnemonic representations across multiple cognitive domains, linking the perceptual world with declarative-memory systems in the human brain.

APPENDIX A.

Category	*Index*	*Target*	*Foil*
abstract	prediction	foresight	loyalty
abstract	upkeep	preservation	weekend
abstract	internship	employee	hindrance
abstract	solution	dilemma	voyage
abstract	luck	lottery	honor
abstract	skill	vocation	strife
abstract	creed	dogma	budget
abstract	greed	wealth	paradox
abstract	analogy	metaphor	menace
abstract	crime	bribe	origin
abstract	chore	task	cult
abstract	motive	behavior	enigma
abstract	burden	affliction	sequel
abstract	charity	donation	pact
abstract	testimony	perjury	fetish
abstract	merit	qualification	pacifism
abstract	synopsis	anecdote	allegory
abstract	saga	epic	proxy
abstract	apathy	malaise	protocol
abstract	fate	soul	gist
abstract	satire	drama	fraud
abstract	guilt	grief	heir
auditory	engine	propeller	rattlesnake
auditory	thunder	downpour	rocket
auditory	choir	orchestra	waterfall
auditory	parrot	rooster	airplane
auditory	dog	wolf	jet

APPENDIX A. (*continued*)

Category	*Index*	*Target*	*Foil*
auditory	siren	ambulance	festival
auditory	lullaby	baby	volcano
auditory	alarm	buzzer	symphony
auditory	applause	speech	avalanche
auditory	fireworks	celebration	subway
auditory	singer	jukebox	storm
auditory	opera	musician	heartbeat
auditory	dialogue	conversation	chime
auditory	stereo	television	infant
auditory	riot	uproar	melody
auditory	cricket	cicada	concert
auditory	belch	hiccup	noise
auditory	ruckus	commotion	narration
auditory	gunshot	dynamite	song
auditory	circus	laughter	carol
auditory	foghorn	ocean	arcade
auditory	utterance	announcement	melody
manipulable	pencil	crayon	spoon
manipulable	hairbrush	comb	clay
manipulable	syringe	scalpel	cigar
manipulable	key	doorknob	shoelace
manipulable	fork	chopsticks	drumstick
manipulable	chisel	screwdriver	lipstick
manipulable	shovel	pitchfork	lighter
manipulable	sword	spear	cup
manipulable	calculator	computer	utensil
manipulable	chess	checkers	corkscrew
manipulable	spatula	ladle	camera
manipulable	cigarette	pipe	handle
manipulable	tissue	handkerchief	flashlight
manipulable	axe	hatchet	tape
manipulable	wheelchair	crutch	knife
manipulable	razor	brush	kite
manipulable	chalk	eraser	dart
manipulable	rope	knot	tool
manipulable	scissors	stapler	arrow
manipulable	paperclip	thumbtack	dough
manipulable	soap	sponge	cane
manipulable	ball	toy	lever

APPENDIX A. (*continued*)

Category	*Index*	*Target*	*Foil*
visual	carrot	potato	lightbulb
visual	penguin	turtle	blueberry
visual	building	elevator	tombstone
visual	diamond	gold	lake
visual	lemon	pineapple	scorpion
visual	corn	sandwich	raft
visual	balloon	confetti	zebra
visual	trophy	ribbon	apple
visual	necklace	bracelet	broccoli
visual	raincoat	parka	crown
visual	cactus	tree	brick
visual	tent	igloo	tire
visual	newspaper	magazine	noodle
visual	snail	slug	bread
visual	pyramid	desert	salad
visual	mountain	boulder	chocolate
visual	fence	lawn	peach
visual	chimney	roof	refrigerator
visual	candle	lantern	daffodil
visual	lamp	sofa	gravel
visual	submarine	whale	cupcake
visual	trashcan	dumpster	butterfly

Reprint requests should be sent to Michael F. Bonner or Murray Grossman, Department of Neurology-2 Gibson, University of Pennsylvania, 3400 Spruce Street, Philadelphia, PA 19104, or via e-mail: michafra@mail.med.upenn.edu, mgrossma@mail.med.upenn.edu.

REFERENCES

Aminoff, E. M., Kveraga, K., & Bar, M. (2013). The role of the parahippocampal cortex in cognition. *Trends in Cognitive Sciences, 17,* 379–390.

Ashburner, J., & Friston, K. (1997). Multimodal image coregistration and partitioning—A unified framework. *Neuroimage, 6,* 209–217.

Ashburner, J., & Friston, K. J. (2005). Unified segmentation. *Neuroimage, 26,* 839–851.

Avants, B. B., Epstein, C. L., Grossman, M., & Gee, J. C. (2008). Symmetric diffeomorphic image registration with cross-correlation: Evaluating automated labeling of elderly and neurodegenerative brain. *Medical Image Analysis, 12,* 26–41.

Barense, M. D., Henson, R. N., & Graham, K. S. (2011). Perception and conception: Temporal lobe activity during complex discriminations of familiar and novel faces and objects. *Journal of Cognitive Neuroscience, 23,* 3052–3067.

Binder, J., & Desai, R. (2011). The neurobiology of semantic memory. *Trends in Cognitive Sciences, 15,* 527–536.

Binder, J., Desai, R., Graves, W., & Conant, L. (2009). Where is the semantic system? A critical review and meta-analysis of 120 functional neuroimaging studies. *Cerebral Cortex, 19,* 2767–2796.

Binder, J. R., Westbury, C. F., McKiernan, K. A., Possing, E. T., & Medler, D. A. (2005). Distinct brain systems for processing concrete and abstract concepts. *Journal of Cognitive Neuroscience, 17,* 905–917.

Bird, C. M., & Burgess, N. (2008). The hippocampus and memory: Insights from spatial processing. *Nature Reviews Neuroscience, 9,* 182–194.

Bonner, M. F., Ash, S., & Grossman, M. (2010). The new classification of primary progressive aphasia into semantic, logopenic, or nonfluent/agrammatic variants. *Current Neurology and Neuroscience Reports, 10,* 484–490.

Bonner, M. F., & Grossman, M. (2012). Gray matter density of auditory association cortex relates to knowledge of sound concepts in primary progressive aphasia. *Journal of Neuroscience, 32,* 7986–7991.

Bonner, M. F., Peelle, J. E., Cook, P. A., & Grossman, M. (2013). Heteromodal conceptual processing in the angular gyrus. *Neuroimage, 71,* 175–186.

Bonner, M. F., Vesely, L., Price, C., Anderson, C., Richmond, L., Farag, C., et al. (2009). Reversal of the concreteness effect in semantic dementia. *Cognitive Neuropsychology, 26,* 568–579.

Breedin, S. D., Saffran, E. M., & Coslett, H. B. (1994). Reversal of the concreteness effect in a patient with semantic dementia. *Cognitive Neuropsychology, 11,* 617–660.

Buckner, R. L., & Carroll, D. C. (2007). Self-projection and the brain. *Trends in Cognitive Sciences, 11,* 49–57.

Bussey, T. J., & Saksida, L. M. (2007). Memory, perception, and the ventral visual-perirhinal-hippocampal stream: Thinking outside of the boxes. *Hippocampus, 17,* 898–908.

Caramazza, A., Anzellotti, S., Strnad, L., & Lingnau, A. (2014). Embodied cognition and mirror neurons: A critical assessment. *Annual Review of Neuroscience, 37,* 1–15.

Chatterjee, A. (2010). Disembodying cognition. *Language and Cognition, 2,* 79–116.

Coltheart, M. (1981). The MRC psycholinguistic database. *Quarterly Journal of Experimental Psychology, 33,* 497–505.

Csernansky, J. G., Gillespie, S. K., Dierker, D. L., Anticevic, A., Wang, L., Barch, D. M., et al. (2008). Symmetric abnormalities in sulcal patterning in schizophrenia. *Neuroimage, 43,* 440–446.

Fairhall, S. L., & Caramazza, A. (2013). Brain regions that represent amodal conceptual knowledge. *Journal of Neuroscience, 33,* 10552–10558.

Fernandino, L., Binder, J. R., Desai, R. H., Pendl, S. L., Humphries, C. J., Gross, W. L., et al. (2015). Concept representation reflects multimodal abstraction: A framework for embodied semantics. *Cerebral Cortex*. doi: 10.1093/cercor/bhv020.

Folstein, M. F., Folstein, S. F., & McHugh, P. R. (1975). "Mini Mental State." A practical method for grading the cognitive state of patients for the clinician. *Journal of Psychiatric Research, 12,* 189–198.

Francis, W. N., & Kucera, H. (1982). *The frequency analysis of English usage*. Boston: Houghton-Mifflin Co.

Friston, K. J., Ashburner, J., Frith, C. D., Poline, J. B., Heather, J. D., & Frackowiak, R. S. J. (1995). Spatial registration and normalization of images. *Human Brain Mapping, 3,* 165–189.

Gilhooly, K. J., & Logie, R. H. (1980). Age-of-acquisition, imagery, concreteness, familiarity, and ambiguity measures

for 1,944 words. *Behavior Research Methods & Instrumentation, 12,* 395–427.
Gorno-Tempini, M. L., Hillis, A. E., Weintraub, S., Kertesz, A., Mendez, M., Cappa, S. F., et al. (2011). Classification of primary progressive aphasia and its variants. *Neurology, 76,* 1006–1014.
Grossman, M. (2010). Primary progressive aphasia: Clinicopathological correlations. *Nature Reviews Neurology, 6,* 88–97.
Hassabis, D., & Maguire, E. A. (2009). The construction system of the brain. *Philosophical Transactions of the Royal Society, Series B, Biological Sciences, 364,* 1263–1271.
Hill, J., Inder, T., Neil, J., Dierker, D., Harwell, J., & Van Essen, D. (2010). Similar patterns of cortical expansion during human development and evolution. *Proceedings of the National Academy of Sciences, U.S.A., 107,* 13135–13140.
Hodges, J. R., & Patterson, K. (2007). Semantic dementia: A unique clinicopathological syndrome. *Lancet Neurology, 6,* 1004–1014.
Hodges, J. R., Patterson, K., Oxbury, S., & Funnell, E. (1992). Semantic dementia: Progressive fluent aphasia with temporal lobe atrophy. *Brain, 115,* 1783–1806.
Hoffman, P., Jones, R. W., & Ralph, M. A. (2012). The degraded concept representation system in semantic dementia: Damage to pan-modal hub, then visual spoke. *Brain, 135,* 3770–3780.
Hoffman, P., & Lambon Ralph, M. A. (2011). Reverse concreteness effects are not a typical feature of semantic dementia: Evidence for the hub-and-spoke model of conceptual representation. *Cerebral Cortex, 21,* 2103–2112.
Howard, D., & Patterson, K. (1992). *Pyramids and palm trees: A test of semantic access from pictures and words*. Bury St. Edmonds, UK: Thames Valley Test Co.
Kanai, R., & Rees, G. (2011). The structural basis of inter-individual differences in human behaviour and cognition. *Nature Reviews Neuroscience, 12,* 231–242.
Kemmerer, D., Castillo, J. G., Talavage, T., Patterson, S., & Wiley, C. (2008). Neuroanatomical distribution of five semantic components of verbs: Evidence from fMRI. *Brain and Language, 107,* 16–43.
Khaligh-Razavi, S.-M., & Kriegeskorte, N. (2014). Deep supervised, but not unsupervised, models may explain IT cortical representation. *PLoS Computational Biology, 10,* e1003915.
Kravitz, D. J., Saleem, K. S., Baker, C. I., Ungerleider, L. G., & Mishkin, M. (2013). The ventral visual pathway: An expanded neural framework for the processing of object quality. *Trends in Cognitive Sciences, 17,* 26–49.
Lambon Ralph, M. A., Cipolotti, L., Manes, F., & Patterson, K. (2010). Taking both sides: Do unilateral anterior temporal lobe lesions disrupt semantic memory? *Brain, 133,* 3243–3255.
Lambon Ralph, M. A., McClelland, J. L., Patterson, K., Galton, C. J., & Hodges, J. R. (2001). No right to speak? The relationship between object naming and semantic impairment: Neuropsychological evidence and a computational model. *Journal of Cognitive Neuroscience, 13,* 341–356.
Lavenex, P., Suzuki, W. A., & Amaral, D. G. (2002). Perirhinal and parahippocampal cortices of the macaque monkey: Projections to the neocortex. *Journal of Comparative Neurology, 447,* 394–420.
Leshinskaya, A., & Caramazza, A. (2014). Nonmotor aspects of action concepts. *Journal of Cognitive Neuroscience, 26,* 2863–2879.
Libon, D. J., Rascovsky, K., Gross, R. G., White, M. T., Xie, S. X., Dreyfuss, M., et al. (2011). The Philadelphia Brief Assessment of Cognition (PBAC): A validated screening measure for dementia. *Clinical Neuropsychologist, 25,* 1314–1330.
Mahon, B. Z., Anzellotti, S., Schwarzbach, J., Zampini, M., & Caramazza, A. (2009). Category-specific organization in the human brain does not require visual experience. *Neuron, 63,* 397–405.
Martin, A. (2007). The representation of object concepts in the brain. *Annual Review of Psychology, 58,* 25–45.
Mion, M., Patterson, K., Acosta-Cabronero, J., Pengas, G., Izquierdo-Garcia, D., Hong, Y. T., et al. (2010). What the left and right anterior fusiform gyri tell us about semantic memory. *Brain, 133,* 3256–3268.
Murray, E. A., Bussey, T. J., & Saksida, L. M. (2007). Visual perception and memory: A new view of medial temporal lobe function in primates and rodents. *Annual Review of Neuroscience, 30,* 99–122.
Nichols, T. E., & Holmes, A. P. (2002). Nonparametric permutation tests for functional neuroimaging: A primer with examples. *Human Brain Mapping, 15,* 1–25.
Paivio, A. (1991). *Images in mind: The evolution of a theory*. Hertfordshire, UK: Harvester Wheatsheaf.
Paivio, A., Yuille, J. C., & Madigan, S. A. (1968). Concreteness, imagery, and meaningfulness: Values for 925 nouns. *Journal of Experimental Psychology, 76,* 125.
Patterson, K., Nestor, P., & Rogers, T. (2007). Where do you know what you know? The representation of semantic knowledge in the human brain. *Nature Reviews Neuroscience, 8,* 976–987.
Peelen, M. V., & Caramazza, A. (2012). Conceptual object representations in human anterior temporal cortex. *Journal of Neuroscience, 32,* 15728–15736.
Peelle, J. E., Cusack, R., & Henson, R. N. (2012). Adjusting for global effects in voxel-based morphometry: Gray matter decline in normal aging. *Neuroimage, 60,* 1503–1516.
Price, A. R., Bonner, M. F., Peelle, J. E., & Grossman, M. (2015). Converging evidence for the neuroanatomic basis of combinatorial semantics in the angular gyrus. *Journal of Neuroscience, 35,* 3276–3284.
Reilly, J., Peelle, J. E., Garcia, A., & Crutch, S. J. (in press). Linking somatic and symbolic representation in semantic memory: The dynamic multilevel reactivation framework. *Psychonomic Bulletin and Review*.
Sabsevitz, D. S., Medler, D. A., Seidenberg, M., & Binder, J. R. (2005). Modulation of the semantic system by word imageability. *Neuroimage, 27,* 188–200.
Scott, D. W. (2015). *Multivariate density estimation: Theory, practice, and visualization*. Hoboken, NJ: John Wiley & Sons.
Scoville, W. B., & Milner, B. (1957). Loss of recent memory after bilateral hippocampal lesions. *Journal of Neurology, Neurosurgery and Psychiatry, 20,* 11–21.
Sha, L., Haxby, J. V., Abdi, H., Guntupalli, J. S., Oosterhof, N. N., Halchenko, Y. O., et al. (2014). The animacy continuum in the human ventral vision pathway. *Journal of Cognitive Neuroscience, 27,* 1–14.
Skipper, L. M., & Olson, I. R. (2014). Semantic memory: Distinct neural representations for abstractness and valence. *Brain and Language, 130,* 1–10.
Stansbury, D., Naselaris, T., & Gallant, J. (2013). Natural scene statistics account for the representation of scene categories in human visual cortex. *Neuron, 79,* 1025–1034.
Suzuki, W. A. (1996). Neuroanatomy of the monkey entorhinal, perirhinal and parahippocampal cortices: Organization of cortical inputs and interconnections with amygdala and striatum. *Seminars in Neuroscience, 8,* 3–12.
Suzuki, W. L., & Amaral, D. G. (1994). Perirhinal and parahippocampal cortices of the macaque monkey: Cortical

afferents. *Journal of Comparative Neurology, 350,* 497–533.
Thompson-Schill, S. L., Aguirre, G., D'Esposito, M., & Farah, M. J. (1999). A neural basis for category and modality specificity of semantic knowledge. *Neuropsychologia, 37,* 671–676.
Tustison, N. J., Avants, B. B., Cook, P. A., Yuanjie, Z., Egan, A., Yushkevich, P. A., et al. (2010). N4ITK: Improved N3 bias correction. *IEEE Transactions on Medical Imaging, 29,* 1310–1320.
Tyler, L. K., Stamatakis, E. A., Bright, P., Acres, K., Abdallah, S., Rodd, J., et al. (2004). Processing objects at different levels of specificity. *Journal of Cognitive Neuroscience, 16,* 351–362.
Van Essen, D. C., Dierker, D., Snyder, A. Z., Raichle, M. E., Reiss, A. L., & Korenberg, J. (2006). Symmetry of cortical folding abnormalities in Williams syndrome revealed by surface-based analyses. *Journal of Neuroscience, 26,* 5470–5483.
Wang, J., Conder, J. A., Blitzer, D. N., & Shinkareva, S. V. (2010). Neural representation of abstract and concrete concepts: A meta-analysis of neuroimaging studies. *Human Brain Mapping, 31,* 1459–1468.
Warrington, E. K. (1975). The selective impairment of semantic memory. *Quarterly Journal of Experimental Psychology, 27,* 635–657.
Wise, R. J. S., Howard, D., Mummery, C. J., Fletcher, P., Leff, A., Büchel, C., et al. (2000). Noun imageability and the temporal lobes. *Neuropsychologia, 38,* 985–994.
Worsley, K. J., Evans, A. C., Marrett, S., & Neelin, P. (1992). A three-dimensional statistical analysis for CBF activation studies in human brain. *Journal of Cerebral Blood Flow and Metabolism, 12,* 900–918.